

# Accreting Fluids onto Regular Black Holes Via Hamiltonian Approach

Abdul Jawad<sup>1</sup> \*and M.Umair Shahzad<sup>1,2</sup> †

<sup>1</sup>Department of Mathematics, COMSATS Institute of Information Technology, Lahore-54000, Pakistan.

<sup>2</sup>CAMS, UCP Business School, University of Central Punjab, Lahore, Pakistan

## Abstract

We investigate the accretion of test fluids onto regular black holes such as Kehagias-Sfetsos black hole and a regular black hole with Dagum Distribution Function. We analyze the accretion process when different test fluids are falling onto these regular black holes. The accreting fluid is being classified through equation of state according to features of regular black holes. The behavior of fluid flow and the existence of sonic points is being checked for these regular black holes. It is noted that three velocity depends on critical points and equation of state parameter on phase space.

## 1 Introduction

A very interesting physical phenomena in astrophysics is the accretion of fluids onto a black hole (BH), which has been rigorously discussed in the literature. The presence of event horizon is distinctive feature of BH which act as one way membrane through which accreting fluid or gas disappears and leads to several important issues. For instance, radiations emitted near the BH undergo the effect of strong gravitational lensing and appears as

---

\*jawadab181@yahoo.com; abduljawad@ciitlahore.edu.pk

†m.u.shahzad@ucp.edu.pk

the image of BH's shadow surrounded by sharp light ring. However, no inner boundary conditions are necessary for equation of motion in case of BH accretion [1]. On the other hand, one of the major challenge in general relativity is the existence of essential singularities and it looks like the common property in most of solutions of Einstein field equations.

Moreover, regular black holes (RBHs) have been constructed to resolve this problem because their metrics are regular everywhere and hence essential singularities can be avoided in the solutions of Einstein equations of BHs physics [2]. These RBHs satisfied the weak energy condition while some of them violate the strong energy conditions [3, 4]. However, Penrose cosmic censorship conjecture claims that singularities predicted by general relativity occur and **they must be enclosed by event horizon** [5, 6]. In this way, Bardeen [7] made the pioneer work and obtained a BH solution without any essential singularity at origin enclosed by event horizon known as 'Bardeen Black Hole' which satisfy weak energy condition. Later, many authors found similar solution [8, 9, 10]. The coupling of general relativity to non-linear electromagnetic theory has brought a new sets of charged RBHs. Hayward [11] and Berej et. al [12] found different kinds of RBH solutions. Recently, Leonardo et. al [13] used various distribution functions (such as logistic, Fermi-Dirac, Dagum etc.) in order to obtain charged RBH. Kehagias-Sftesos (KS) found asymptotically flat RBH which usually behaves like Schwarzschild (SH) BH in Horava theory [14].

The pioneer work on accretion for spherical symmetry was introduced by Bondi in the frame work of Newtonian gravity [15]. Many authors have investigated Bondi-type accretion flows in SH, SH de-Sitter and SH anti-de-Sitter BHs [16, 17, 18]. In this extension, Michel [19] proposed its general relativistic version by considering the steady state flow of perfect fluid onto BH along the radial direction. The stability of Michel type accretion in subsonic region has been analyzed by Moncrief [20]. Further, it was suggested by Babichev et al. [21] that BH loses its mass during the accretion of phantom dark energy onto it. Furthermore, many authors have worked on radial flows such as accretion of dark matter onto BH [22], radial accretion onto cosmological BHs [16, 17], for self gravitating [23, 24] and perturbation theories [25]. The accretion onto Einstein - Maxwell - Gauss - Bonnet BH and topologically charged BHs in  $f(R)$  theories has been presented in [26, 27]. The nonlinear study of phantom scalar field accreted onto a BH was done Gonzalez and Guzman [28] with the help of numerical methods. In this direction, some works have been done by various people [29, 30, 2] and showed that

when phantom-like fluids accrete onto BHs/RBHs then mass of BHs/RBHs decrease, respectively.

Recently, Chaverra et al. [1] and Ahmed et al. [31, 32] have discussed Michel-type accretion near SH,  $f(R)$  and  $f(T)$  BHs. In the present work, we will use similar technique in order to discuss the accretion onto well-known RBHs. Rest of the paper is organized as follows: In section 2, we derive general formalism for spherically static accretion process. In section 3, we discuss the accretion process using Hamiltonian dynamical system and study the system at sonic points. In section 4, we study two RBHs: KS-BH and RBH using Dagum Distribution Function (DDF RBH). In section 5, we find the solutions for isothermal test fluids of each RBH for different kinds of fluids. In section 6, we investigate the accretion phenomena for polytropic fluid. In the last section, we summarize our results.

## 2 General equations of spherical accretion

Here, we will derive the governing equations and analyze the flow of perfect fluid and accretion rate onto RBHs by utilizing the energy and particle conservation laws. In this way, we consider general spherical symmetric and stationary line element as follows

$$ds^2 = -X(r)dt^2 + \frac{1}{X(r)}dr^2 + r^2(d\theta^2 + \sin^2\theta d\phi^2), \quad (1)$$

where  $X(r) > 0$  is the function of  $r$ . The energy momentum tensor for perfect fluid is given by

$$T_{\mu\nu} = (p + \varepsilon)u_\mu u_\nu + pg_{\mu\nu}, \quad (2)$$

where  $p$  is the pressure,  $\varepsilon$  is the energy density and  $u^\mu$  is the four velocity which is given by

$$u^\mu = \frac{dx^\mu}{d\tau} = (u^t, u^r, 0, 0), \quad (3)$$

where  $\tau$  is the proper time. Here,  $u^\theta$  and  $u^\phi$  become zero due to spherical symmetry restrictions. We define the current density or particle flux by  $J^\mu = nu^\mu$ . According to law of particle conservation, the divergence of particle flux is zero for this system, i.e.,

$$\nabla_\mu J^\mu = \nabla_\mu(nu^\mu) = 0, \quad (4)$$

where  $\nabla_\mu$  is covariant derivative. It is useful to mention here that all the flow variables  $(p, \varepsilon, u^\mu, n)$  are spherically symmetric and steady state according to definition of Michel [16, 17]. Using Eq.(1) and normalization condition  $u^\mu u_\mu = -1$ , we have

$$u_t = \pm \sqrt{u^2 + X(r)}. \quad (5)$$

where  $u = dr/d\tau = u^r$ ,  $u^t$  can be negative or positive due to square root which represents the backward or forward in time conditions. However,  $u < 0$  is required for accretion process otherwise for any outward flows  $u > 0$ . The equation of continuity is

$$\nabla_\mu(nu^\mu) = \frac{1}{r^2} \partial_r(r^2 nu) = 0, \quad (6)$$

which leads to

$$r^2 nu = C_a, \quad (7)$$

where  $C_a$  is integration constant. The thermodynamics of perfect fluid is given by [33]

$$dp = n(dh - Tds), \quad d\varepsilon = hdn + nTds, \quad (8)$$

where  $h = \frac{\varepsilon + p}{n}$  is the specific enthalpy,  $T$  is the temperature and  $s$  is the specific entropy.

Furthermore, the theorem of relativistic hydrodynamics (which is only applicable for smooth flows) states that the scalar quantities such as  $hu_\mu \eta^\mu$  remain conserved along the trajectories of the fluid [33], i.e.,

$$u^\nu \partial_\mu(hu_\mu \eta^\mu) = 0, \quad (9)$$

where  $\eta^\mu$  is a Killing vector of space-time. Considering  $\eta^\mu = (1, 0, 0, 0)$  of metric (1), we obtain

$$h\sqrt{u^2 + X(r)} = C_b \quad (10)$$

where  $C_b$  is integration constant. It is also mention here that the specific entropy remains conserved along the fluid trajectories, i.e.,  $u^\mu \nabla_\mu s = 0$ . Hence, the stress energy tensor  $T_{\mu\nu}$  can be written as [31, 32]

$$T_{\mu\nu} = nhu_\mu u_\nu + (nh - \varepsilon)g_{\mu\nu}$$

and then projection of  $T^{\mu\nu}$  onto  $u^\mu$  turns out to be

$$u_\nu \nabla_\mu T^{\mu\nu} = u_\nu \nabla_\mu [nhu_\mu u_\nu + (nh - \varepsilon)g_{\mu\nu}] = -nT u^\mu \nabla_\mu s = 0. \quad (11)$$

Since fluid is stationary (independent of time) and moving along radial direction only in the present case which leads to  $\partial_r s = 0$  and hence  $s$  becomes constant. In this scenario, Eq. (8) reduces to

$$dp = ndh, \quad d\varepsilon = hdn. \quad (12)$$

Next, we will use Eqs.(7), (10) and (12) to analyze the flow. Since  $s$  becomes constant and thus canonical form of EoS of simple fluid ( $\varepsilon = \varepsilon(n, s)$ ) [31, 32] turns out to be barotropic form and is given by

$$\varepsilon = F(n). \quad (13)$$

In view of above relation, Eq.(12) leads to

$$h = \frac{d\varepsilon}{dn} = \frac{dF(n)}{dn} = F'(n), \quad p' = nF'' \implies p = nF' - F, \quad (14)$$

which provides the relationship between  $F$  and  $G$  ( $p = G(n)$ ) as follows

$$G(n) = nF'(n) - F(n). \quad (15)$$

Further, the sound speed can be defined as  $a^2 = (\partial p / \partial \varepsilon)_s$ , which reduces to  $a^2 = dp/d\varepsilon$  because  $s$  is constant. Using (12), we can find

$$\frac{dh}{h} = a^2 \frac{dn}{n}. \quad (16)$$

Using Eqs.(14) and (16), we obtain

$$a^2 = n(\ln F')'. \quad (17)$$

Since the motion is in radial direction, so the metric (1) reduces to

$$ds^2 = -(\sqrt{X(r)}dt)^2 + \left( \frac{dr}{\sqrt{X(r)}} \right)^2. \quad (18)$$

The ordinary three velocity of the fluid can be defined as  $v \equiv \frac{dr/\sqrt{X(r)}}{\sqrt{X(r)}dt}$  and its expression can be obtained by using relations  $u^t = dt/d\tau$ ,  $u = u^r = dr/d\tau$ ,  $u_t = -X(r)u^t$  and Eq.(5) as follows

$$v^2 = \frac{u^2}{X(r) + u^2}, \quad (19)$$

which implies

$$u^2 = \frac{X(r)v^2}{1-v^2} \quad \text{and} \quad (u_t)^2 = \frac{X^2(r)}{1-v^2}. \quad (20)$$

Utilizing above relations in (7), we obtain

$$C_a^2 = \frac{r^4 n^2 X(r) v^2}{1-v^2}. \quad (21)$$

These results will be used in the following sections [31, 32].

### 3 Hamiltonian system

Here, we derive two integrals of motion ( $C_a, C_b$ ) given in (7) and (10) by adopting Hamiltonian procedure. The idea of reformulating of the Michel flow problem as a Hamiltonian system for global flow is analyzed in detail by [1, 34, 35, 36]. The Hamiltonian  $H$  is a function of two variables ( $x, y$ ) and its simplest form has one degree of freedom. Let  $H$  be the square of L.H.S of Eq.(10):

$$H = h^2(X(r) + u^2). \quad (22)$$

Using Eq.(20) in above equation, we have

$$H(r, v) = \frac{h(r, v)^2 X(r)}{1-v^2}, \quad (23)$$

and this is derived in [31, 32]. Here, we fixed dynamical variables to be ( $r, v$ ). For the derivation of critical points, particularly, the sonic points are derived in following subsection.

#### 3.1 Sonic points

The dynamical system of Hamiltonian  $H$  given in (23) reads to be [31, 32]

$$\dot{v} = -H_{,r}, \quad \dot{r} = H_{,v}, \quad (24)$$

where dot represents the derivative with respect to  $\bar{t}$  which is new **"time"** variable. The **"time"** variable  $\bar{t}$  for the dynamical system is any variable on which Eq. (22) does not depend explicitly so that the dynamical system is

autonomous. For finding critical points (CPs), we utilize Eq.(24) for which we require

$$\frac{d}{dr}H(r, v) = \frac{h^2}{1-v^2} \left( \frac{d}{dr}(X(r)) + 2X(r)\frac{d}{dr}(\ln h) \right), \quad (25)$$

$$\frac{d}{dv}H(r, v) = \frac{2X(r)h^2v}{(1-v^2)^2} \left( 1 + \frac{1-v^2}{v^2} \frac{d}{dv}(\ln h) \right). \quad (26)$$

Moreover, Eq.(16) can be expressed as

$$\frac{d}{dr}(\ln h) = a^2 \frac{d}{dr}(\ln n), \quad (27)$$

$$\frac{d}{dv}(\ln h) = a^2 \frac{d}{dv}(\ln n). \quad (28)$$

By keeping 'r' as a constant in Eq.(21), we have  $\frac{nv}{\sqrt{1-v^2}} = \text{constant}$  which under differentiation w.r.t. 'v' leads to

$$\frac{d}{dv}(\ln n) = -\frac{1}{v(1-v^2)} \Rightarrow \frac{d}{dv}(\ln h) = -\frac{a^2}{v(1-v^2)}. \quad (29)$$

Similarly,

$$\frac{d}{dr}(\ln n) = -\frac{4 + r \frac{d}{dr}(\ln X(r))}{2r} \Rightarrow \frac{d}{dr}(\ln h) = -\frac{a^2(4 + r \frac{d}{dr}(\ln X(r)))}{2r}. \quad (30)$$

Finally, by using Eqs.(24)-(30), we obtain

$$\dot{v} = -\frac{h^2}{r(1-v^2)} \left( r \left( \frac{d}{dr}X(r) \right) (1-a^2) - 4X(r)a^2 \right), \quad (31)$$

$$\dot{r} = -\frac{2X(r)h^2}{v(1-v^2)^2} (v^2 - a^2). \quad (32)$$

By setting the above relations equal to zero, we can get CPs as follows

$$v_c^2 = a_c^2 \quad \text{and} \quad r_c(1-a_c^2) \frac{d}{dr_c}X(r_c) = 4X_c a_c^2. \quad (33)$$

Here  $X_c \equiv X(r_c)$  and  $\frac{d}{dr_c}X_c \equiv \frac{d}{dr}X(r) \big|_{r=r_c}$ . The second relation of Eq.(33) represents the sound speed at the CP, i.e.,  $a_c^2$  in terms of  $r_c$

$$a_c^2 = \frac{r_c \frac{d}{dr_c}X_c}{4X_c + r_c \frac{d}{dr_c}X_c}, \quad (34)$$

In this scenario, the constant  $C_a^2$  (21) can be written as

$$C_a^2 = r_c^4 n_c^2 v_c^2 \frac{X_c}{1 - v_c^2} = \frac{1}{4} r_c^5 n_c^2 \frac{d}{dr_c} X_c, \quad (35)$$

where we have used (33). Using  $C_a^2$  in Eq.(21), we have

$$\left(\frac{n}{n_c}\right)^2 = \frac{r_c^5 \left(\frac{d}{dr_c} X_c\right) (1 - v^2)}{4r^4 X(r) v^2}. \quad (36)$$

## 4 Regular Black holes

In this section, we will discuss RBHs with fixed BH background, neglecting the self-gravity of the fluid.

### 4.1 KS Regular Black hole

Recently, Horava proposed the renormalizable gravity theory with higher order spatial derivatives in four dimensional space-time. **It is an ultra-violet completion of general relativity. This theory reduces to Einstein gravity with non-vanishing cosmological constant under infrared limit, but it has improved ultraviolet behaviors.** Moreover, in deformed Horava-Lifshitz (HL) gravity, the ultraviolet properties are unchanged, whereas there exists a Minkowski vacuum in infra-red limit. The HL theory is considered as very interesting and many researchers discovered new BH solutions after its formulation [37, 14, 38, 39]. Many new aspects discussed in connection with HL theory [40]. The metric function of KS RBH in deformed HL gravity is given by

$$X(r) = 1 + br^2 \left(1 - \sqrt{1 + \frac{4M}{br^3}}\right), \quad (37)$$

where  $b$  is the arbitrary constant and  $M$  is BH mass. However, the constraints on the value of  $bM^2$  have been developed through the comparison of perihelion shift test of KS BH with the observations in the solar system. It was found that  $bM^2 \geq 1.7 \times 10^{-12}$  for Saturn,  $bM^2 \geq 9 \times 10^{-12}$  for Mars and  $bM^2 \geq 7.2 \times 10^{-10}$  for Mercury [41]. KS BH can be reduced to  $X(r) = 1 - \frac{2M}{r} + \frac{2M^2}{br^4} + \dots$  in the limiting case  $b \rightarrow \infty$  or  $r \rightarrow \infty$ , while

asymptotically behaves as the SH metric. The infra-red properties of KS and RN BHs are different as shown in third term of expansion [42]. The KS metric have two horizons  $r_h$  (outer) and  $r_{ch}$  (inner) and can be obtained from the metric function (37) as follows

$$r_{ch} = M \left( 1 - \sqrt{\left(1 - \frac{1}{2bM^2}\right)} \right) \quad \text{and} \quad r_h = M \left( 1 + \sqrt{\left(1 - \frac{1}{2bM^2}\right)} \right), \quad (38)$$

with  $2bM^2 \geq 1$  [43]. For  $2bM^2 = 1$ , we have an extreme BH and for  $2bM^2 < 1$ , we have naked singularity.

## 4.2 Regular Black hole using Dagum Distribution Function

Consider the line element (1) for generally spherically symmetric metric with

$$X(r) = 1 - \frac{2M}{r} \frac{\xi(r)}{\xi(\infty)}, \quad (39)$$

where the Dagum distribution function [44] is

$$\xi(x) = \frac{apx^{ap-1}}{b^{ap} \left(1 + \left(\frac{x}{b}\right)^a\right)^{p+1}}, \quad (40)$$

and  $a, b, p$  are positive parameters. By assuming  $b = 1$  and  $p = 1/a$ , we find

$$\xi(x) = \frac{1}{\left(1 + x^a\right)^{\frac{a+1}{a}}}. \quad (41)$$

After replacing  $x \rightarrow \frac{q^2}{Mr}$  and simplifications leads to

$$X(r) = 1 - \frac{2M}{r} \left( \frac{1}{\left(1 + r \left(\frac{q^2}{Mr}\right)^a\right)^{\frac{a+1}{a}}} \right)^\beta. \quad (42)$$

This BH satisfies the weak energy condition for  $\beta = \frac{3}{a+1}$  and hence we have

$$X(r) = 1 - \frac{2M}{r} \left( \frac{1}{\left(1 + r \left(\frac{q^2}{Mr}\right)^a\right)^a} \right)^{3/a}. \quad (43)$$

Moreover, one can find the RBH metric by using Dagum distribution function with a factor  $q/r^2$  which behaves asymptotically as RN metric and its metric function is

$$X(r) = 1 - \frac{2M}{r} \left( \frac{1}{1 + \gamma \left( \frac{q^2}{Mr} \right)^a} \right)^{\frac{3}{a}} + \frac{q^2}{r^2} \left( \frac{1}{1 + \gamma \left( \frac{q^2}{Mr} \right)^a} \right)^{\frac{4}{a}}, \quad (44)$$

where  $\gamma > 0$  is a constant and  $a \geq 2$  is an integer. It should be noted that the associated solution satisfies the weak energy condition if we have  $\gamma \geq (2/3)^a$  as shown in [45]. The associated electric field expression is given by

$$E = \frac{q}{r^2} \left( \frac{3\gamma(3+a) \left( \frac{q^2}{Mr} \right)^{a-1}}{2 \left( 1 + \gamma \left( \frac{q^2}{Mr} \right)^a \right)^{2+\frac{3}{a}}} + \frac{1 - 3\gamma(3+a) \left( \frac{q^2}{Mr} \right)^a}{\left( 1 + \gamma \left( \frac{q^2}{Mr} \right)^a \right)^{2(2+a)/a}} \right). \quad (45)$$

The metric with function (44) behave-like de Sitter BH metric as

$$X(r) \approx 1 - \frac{M^4}{\gamma^{\frac{4}{a}} q^6} (2\gamma^{\frac{1}{a}} - 1) r^2. \quad (46)$$

It can be noticed that **the term proportional to  $r^2$**  cannot become zero because  $\gamma \geq (2/3)^a$ . The metric function (44) remains regular, if we set  $(1/2)^a \leq \gamma < (2/3)^a$  but they have de Sitter center without satisfying the weak energy condition. Therefore, if BH metric is regular and satisfies the weak energy condition, then it has a de Sitter center [46]. However, if the metric has a de Sitter behavior when approaching to the center, it does not necessarily satisfies the weak energy condition. Furthermore, if we set  $\gamma < (1/2)^a$ , BH metric is not regular. Finally, there is a known case which can be obtained as a particular case of Eq.(44) by choosing  $a = 2$  and  $\gamma = \frac{M^2}{q^2}$ , i.e,

$$X(r) = 1 - \frac{2M \left( \frac{r^2}{r^2+q^2} \right)^{3/2}}{r} + \frac{q^2}{r^2} \left( \frac{r^2}{r^2+q^2} \right)^2. \quad (47)$$

This case corresponds to the RBH metric given in [47] and we will discuss the accretion onto this RBH in the following sections.

## 5 Isothermal test fluids

The fluid flowing at a constant temperature is known as isothermal fluids. In accretion process, sound speed of the fluid flow remains constant. Moreover, the speed of sound at sonic points is equal to the speed of sound of accretion flow at any radius [31]. Here, we follow [32] to find the general solution of isothermal EoS of the form  $p = k\varepsilon$  which leads to  $p = kF(n)$  and  $G(n) = kF(n)$  given in Eqs. (13) and (15), respectively, where  $k$  ( $0 < k \leq 1$ ) is the state parameter. The differential equation (15) becomes

$$nF'(n) - F(n) = kF(n), \quad (48)$$

using (13) and integrating above equation, we have

$$\varepsilon = F = \frac{\varepsilon_c}{n_c^{k+1}} n^{k+1}, \quad (49)$$

where  $\frac{\varepsilon_c}{n_c^{k+1}}$  appears as integration constant and hence Eq.(14) becomes

$$h = \frac{(k+1)\varepsilon_c}{n_c} \left( \frac{n}{n_c} \right)^k. \quad (50)$$

Using Eq.(36), we have

$$h^2 \propto \left( \frac{1-v^2}{v^2 r^4 X(r)} \right)^k, \quad (51)$$

and

$$H(r, v) = \frac{X^{1-k}(r)}{(1-v^2)^{1-k} v^{2k} r^{4k}}, \quad (52)$$

where all constants get absorb in the redefinition of Hamiltonian  $H$  and the time  $\bar{t}$ . Next, we need to discuss the pressure physically. Using EoS  $p = k\varepsilon$  and by substituting Eq.(36) in (49), we get

$$p \propto \left( \frac{1-v^2}{X(r)v^2 r^4} \right)^{\frac{k+1}{2}}. \quad (53)$$

If this pressure approaches to the event horizon from the region where  $t$  is time like, then  $X(r) \rightarrow 0$  and the speed  $v \rightarrow 0$  or  $1$ . In this situation, Hamiltonian remains constant on the solution curve. For  $v \rightarrow 0$ , the solution curve approaches to horizon and hence pressure diverges. For  $v \rightarrow 1$ , Eq.

(53) remains finite in the surrounding of horizon [31, 32]. If  $X(r) = 0$  has single root as  $r \rightarrow r_h$  then using (53), one can observe the pressure diverges as

$$p \sim (r - r_h)^{-\frac{k+1}{2k}}. \quad (54)$$

If  $X(r) = 0$  has double root then

$$p \sim (r - r_h)^{-\frac{k+1}{k}}. \quad (55)$$

The Hamiltonian (52) of the dynamical system is a constant along the solution curve. A global flow solution that extends to spatial infinity is

$$v \simeq v_1 r^{-\alpha} + v_\infty \text{ as } r \rightarrow \infty, \quad (56)$$

where  $(v_1, |v_\infty| \leq 1, \alpha > 0)$  are constants. Substituting Eq. (56) in Hamiltonian (52), we obtain

$$H \simeq \frac{X^{1-k}(r)}{r^{4k}} \quad 0 < |v_\infty| < 1, \quad (57)$$

$$H \simeq \frac{X^{1-k}(r)}{r^{(4-2\alpha)k}} \quad |v_\infty| = 0, \quad (58)$$

$$H \simeq \frac{X^{1-k}(r)}{r^{(4k+k\alpha-\alpha)}} \quad |v_\infty| = 1. \quad (59)$$

Now the behavior of the fluid is analyzed by considering different choices of state parameter  $k$  such as  $k = 1/4$  (sub-relativistic fluid),  $k = 1/3$  (radiation fluid),  $k = 1/2$  (ultra-relativistic fluid) and  $k = 1$  (ultra-stiff fluid) and these are discussed in following subsections.

## 5.1 Solution for ultra-stiff fluid ( $k = 1$ )

We assume the fluids with EoS  $p = \epsilon$  and these are ultra-stiff fluids. For instance, the usual EoS for the ultra-stiff fluids is  $p = k\epsilon$ , i.e., the value of state parameter is defined as  $k = 1$ . The Hamiltonian (52) reduces to

$$H = \frac{1}{v^2 r^4}. \quad (60)$$

In this case, the metric function  $X(r)$  does not involve and it is discussed in detail in [1, 31, 32].

## 5.2 Solution for ultra-relativistic fluid ( $k = 1/2$ )

Here, we consider the fluids with EoS  $p = \epsilon/2$  and these fluids are ultra-relativistic. The Hamiltonian takes the simple form

$$H = \frac{\sqrt{X(r)}}{r^2|v|\sqrt{1-v^2}} \quad (61)$$

It is clear from this expression that the point  $(r, v^2) = (r_h, 1)$  is not a critical point of the dynamical system. For some given value of  $H = H_c$ , Eq. (61) can be solved for  $v^2$  as follows

$$v^2 = \frac{1 \pm \sqrt{1 - 4f(r)}}{2} \quad (62)$$

where  $f(r) \equiv \frac{X(r)}{H_c r^4}$ . We plot the above velocity of fluid ( $v$ ) versus  $r$  for aforementioned two RBHs such as KS RBH and DDF RBH by inserting the corresponding values of  $X(r)$  as shown in the left and right panels of Fig. 1, respectively. The trajectories in Fig. 1 corresponds to values of  $H_0 = \{H_c, H_c \pm 0.04, H_c \pm 0.09\}$  where  $H = H_c = 0.170615$  (for KS RBH) and  $H = H_c = 0.170615$  (for DDF RBH). However the values of  $(r_h, r_c, v_c)$  are approximately equal to  $(1.66, 2.1575, 0.707107)$  and  $(1.32, 1.75626, 0.707107)$  for KS RBH and DDF RBH, respectively. For  $H = H_c = 0.170615$  (KS RBH) and  $H = H_c = 0.232518$  (DDF RBH), the solution curves pass through the CPs  $(r_c, -v_c)$  and  $(r_c, v_c)$ . It is observed that the heteroclinic orbit exists in the range  $-v_c < v < v_c$  and also passes through two CPs  $(r_c, -v_c)$  and  $(r_c, v_c)$ . It can also be seen that the fluid flow is closer to DDF RBH instead of KS BH. It is mentioned here that the fluid experiences the particle emission or fluid flow-out when  $v > 0$  while fluid accretes for  $v < 0$ . Moreover, Fig. 1 describes the following four types of fluid.

- We observe the supersonic/subsonic flows out of the fluid in the ranges  $v_c < v < 1$  and  $0 < v < v_c$ , while subsonic/supersonic accretion appear in the ranges  $-v_c < v < 0$  and  $-1 < v < -v_c$ , respectively.
- We have purely supersonic outflow for  $v > v_c$  and purely supersonic accretion for  $v < -v_c$ .
- We have subsonic flow-out followed by subsonic accretion for  $v_c > v > -v_c$ .

- We have supersonic out flow followed by subsonic motion, (upper plot) and subsonic accretion followed by supersonic accretion (lower plot).

According to above discussion, we can say that the fluid outflow starts at horizon because of its high pressure which leads to divergence (can be seen from Eq.(54)) and the fluid under the effects of its own pressure flows back to spatial infinity [32]. From Fig. 1, we observe that the supersonic accretion followed by subsonic accretion and ends inside the horizon which does not give support to the claim that “the flow must be supersonic at the horizon” [48]. Thus, the flow of the fluid is neither transonic nor supersonic near the horizon [49, 50]. These new solutions correspond to fine tuning and instability problems in dynamical systems. The issue of stability is related to the nature of saddle points (CPs  $(r_c, v_c)$  and  $(r_c, -v_c)$ ) of the Hamiltonian function. Further analysis of stability could be done by using Lyapunov’s theorem or linearization of dynamical system [51, 52, 53] and their variations [54]. Another stability issue is the outflow of the fluid starts in the surrounding of horizon under the effect of pressure divergent. This outflow is unstable because it follow a subsonic path passing through the saddle point  $(r_c, v_c)$  and becomes supersonic with speed approaches the speed of the light. The point  $(r = r_h, v = 0)$  can be observed as attractor as well as repeller where solution curves converge and diverge, respectively, in the cosmological point of view [32, 54].

### 5.3 Solutions for $(k = 1/3)$ and $(k = 1/4)$ : Separatrix heteroclinic flows

The EoS with  $k = 1/3$  and  $k = 1/4$  describes the fluid such as photon gas and Sub-relativistic fluids (those fluids whose energy density exceeds their isotropic pressure), respectively. The Hamiltonian (52) for above mentioned fluids takes the following form

$$H = \frac{X^{2/3}(r)}{r^{4/3}|v|^{2/3}(1-v^2)^{2/3}}, \quad \text{for } k = 1/3 \quad (63)$$

$$H = \frac{X^{3/4}(r)}{r|v|^{1/2}(1-v^2)^{3/4}}, \quad \text{for } k = 1/4. \quad (64)$$

It is clear from (63) and (64) that  $(r, v^2) = (r_h, 1)$  are not CPs of dynamical system. Figure 2 represents the contour plots of (63) and (64) in  $(r, v)$

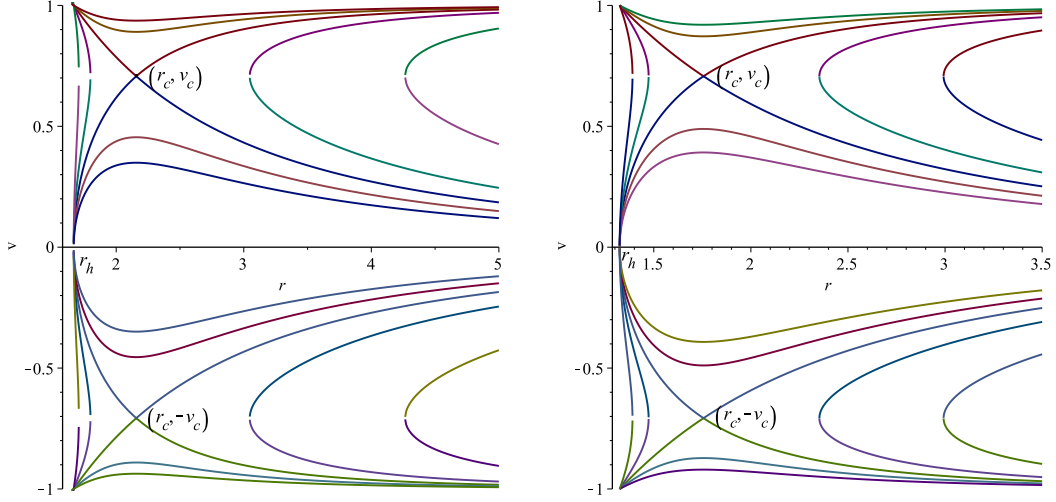


Figure 1: Case  $k = 1/2$ . Left Panel: Plot of (62) for KS BH with  $M = 1$ ,  $b = 0.9$ . Right Panel: Plot of (62) for DDF RBH with  $M = 1$ ,  $q = 0.6$ .

for  $k = 1/3$  (left panel) and  $k = 1/4$  (right panel). We compare the fluid flow for DDF RBH (red plot) and KS RBH (blue plot) in left panel ( $k = 1/3$ ) and right panel ( $k = 1/4$ ). For the case  $k = 1/3$ , there are two saddle points  $(r_{c_1}, -v_{c_1})$  and  $(r_{c_1}, v_{c_1})$  for DDF RBH and two saddle points  $(r_{c_2}, -v_{c_2})$  and  $(r_{c_2}, v_{c_2})$  for KS RBH. It is observed that the subsonic flow proceeds from upper branch in lower plot, passes through CPs  $(r_{c_1}, -v_{c_1})$  (DDF RBH) and  $(r_{c_2}, -v_{c_2})$  (KS RBH), then crosses the horizon  $r_{h_1}$  (DDF RBH) and  $r_{h_2}$  (KS RBH). On the other hand, supersonic flows proceeds from the lower branch in lower plot again passes through the CPs  $(r_{c_1}, -v_{c_1})$  and  $(r_{c_2}, -v_{c_2})$ ; as the fluid approaches the horizon then  $v$  vanishes. The supersonic accretion proceeds from the upper branch of upper plot and passes through CPs  $(r_{c_1}, v_{c_1})$  (DDF RBH) and  $(r_{c_2}, v_{c_2})$  (KS RBH) and so on. For subsonic accretion, fluid proceeds from the lower branch of upper plot and passes through CPs and crosses the horizons. Similar behavior of fluid could be observed for the case  $k = 1/4$  in the right panel of Figure 2.

The left panel of Figure 3 represents the comparison of (63) ( $k = 1/3$ ) and (64) ( $k = 1/4$ ) for KS RBH. It can be seen that if the value of  $k$  increases, then the saddle points shifted towards the KS RBH. Also, the right Panel of Figure 3 represents the comparison of (63) ( $k = 1/3$ ) and (64) ( $k = 1/4$ ) for DDF RBH. Similar behavior of CPs is observed for DDF RBH.

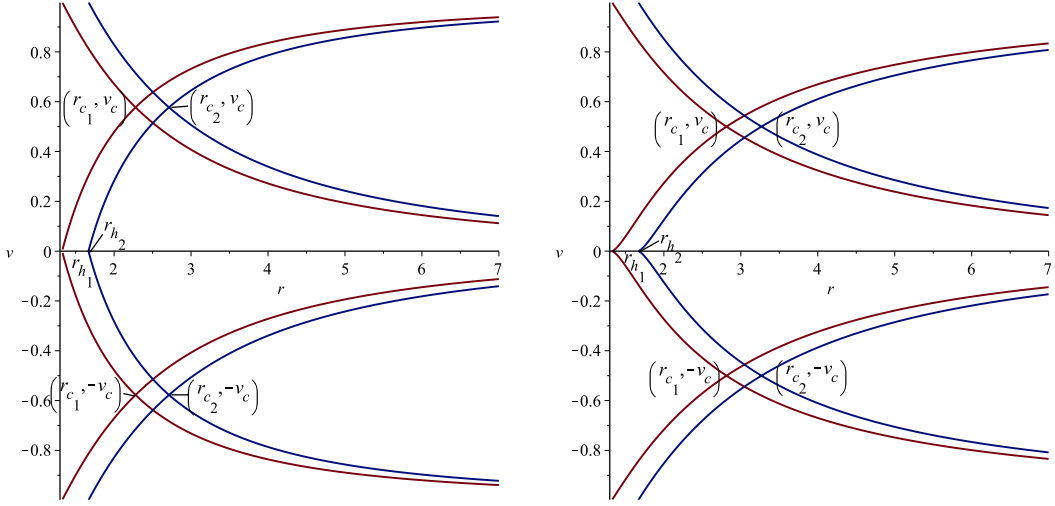


Figure 2: Left panel: Case  $k = 1/3$ . Red plot of (63) for DDF RBH with  $q = 0.6$  and  $M = 1$ . The parameters are  $r_h \simeq 1.33$ ,  $r_{c_1} = 2.2787$  and  $v_c = \frac{1}{\sqrt{3}} \simeq 0.57736$ . The solution curve passes through the saddle CPs  $(r_{c_1}, v_c)$  and  $(r_{c_1}, -v_c)$  for which  $H = H_c \simeq 0.261266$ . Blue plot of (63) for KS RBH with  $b = 0.9$  and  $M = 1$ . The parameters are  $r_h \simeq 1.68$ ,  $r_{c_2} = 2.71329$  and  $v_c = \frac{1}{\sqrt{3}} \simeq 0.57736$ . The solution curve passes through the saddle CPs  $(r_{c_2}, v_c)$  and  $(r_{c_2}, -v_c)$  for which  $H = H_c \simeq 0.22373$ . Right panel: Case  $k \leq 1/4$ . Red plot of (64) for DDF RBH with  $q = 0.6$  and  $M = 1$ . The parameters are  $r_h \simeq 1.367$ ,  $r_{c_1} = 2.81368$  and  $v_c = 0.5$ . The solution curve passes through the saddle CPs  $(r_{c_1}, v_c)$  and  $(r_{c_1}, -v_c)$  for which  $H = H_c \simeq 0.29985$ . Blue plot of (64) for KS RBH with  $b = 0.9$  and  $M = 1$ . The parameters are  $r_h \simeq 1.717$ ,  $r_{c_2} = 3.2682$  and  $v_c = 0.5$ . The solution curve passes through the saddle CPs  $(r_{c_2}, v_c)$  and  $(r_{c_2}, -v_c)$  for which  $H = H_c \simeq 0.273276$ .

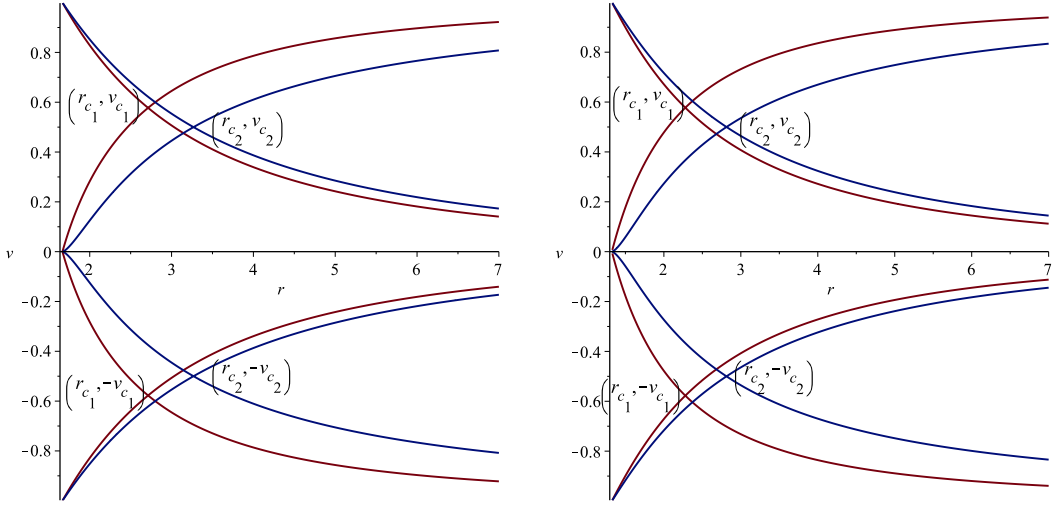


Figure 3: Case  $k \leq 1/3$ . Left panel: Red plot of (63) for KS RBH with  $b = 0.9$  and  $M = 1$  ( $k = 1/3$ ). The parameters are  $r_h \simeq 1.717$ ,  $r_{c_1} = 2.71329$  and  $v_{c_1} = \frac{1}{\sqrt{3}} \simeq 0.57736$ . Blue plot of (64) for KS RBH  $b = 0.9$  and  $M = 1$  ( $k = 1/4$ ). The parameters are  $r_h \simeq 1.717$ ,  $r_{c_2} = 3.2682$  and  $v_{c_2} = 0.5$ . Right panel: Red plot of (63) for DDF RBH with  $q = 0.6$  and  $M = 1$  ( $k = 1/3$ ). The parameters are  $r_h \simeq 1.33$ ,  $r_{c_1} = 2.2787$  and  $v_{c_1} = \frac{1}{\sqrt{3}} \simeq 0.57736$ . Blue plot of (64) for DDF RBH  $b = 0.9$  and  $M = 1$  ( $k = 1/4$ ). The parameters are  $r_h \simeq 1.33$ ,  $r_{c_2} = 2.2787$  and  $v_{c_2} = 0.5$ .

## 6 Polytropic test fluids

The polytropic EoS is

$$p = G(n) = Kn^\alpha, \quad (65)$$

where  $K$  and  $\alpha$  are constants. One can apply the constraint  $\alpha > 1$  for ordinary matter. From Eqs. (15) and (65), one can easily construct the expression of specific enthalpy:

$$h = m + \frac{K\alpha n^{\alpha-1}}{\alpha - 1}, \quad (66)$$

where  $m$  is the baryonic mass. Using above equation and the three dimensional speed of sound (17), we have

$$a^2 = \frac{(\alpha - 1)U}{m(\alpha - 1) + U}, \quad (67)$$

where ( $U \equiv K\alpha n^{\alpha-1}$ ). Equations (66) and (67) leads to

$$h = m \frac{\alpha - 1}{\alpha - 1 - a^2}. \quad (68)$$

Furthermore, using (23) and (66), we have

$$h = m \left( 1 + Q \left( \frac{1 - v^2}{r^4 X(r) v^2} \right)^{(\alpha-1)/2} \right), \quad (69)$$

where

$$Q \equiv \frac{K\alpha n_c^{\alpha-1}}{m(\alpha - 1)} \left( \frac{r_c^5 X(r_c)_{,r_c}}{4} \right)^{\left(\frac{\alpha-1}{2}\right)} = \text{constant}. \quad (70)$$

Inserting (69) into (23), the Hamiltonian system takes the following form

$$H = \frac{X(r)}{1 - v^2} \left( 1 + Q \left( \frac{1 - v^2}{r^4 X(r) v^2} \right)^{\left(\frac{\alpha-1}{2}\right)} \right)^2, \quad (71)$$

where  $m^2$  has been absorbed into a redefinition of  $(\bar{t}, H)$ . It is observed that  $\frac{dX(r)}{dr} > 0$  for all  $r$  which implies that  $Q > 0$  with  $\gamma > 1$ . Hence, the square term in Eq. (71) is positive while the coefficient  $\frac{X(r)}{1-v^2}$  diverges as  $r$  approaches to infinity ( $0 \leq 1 - v^2 < 1$ ). Thus the Hamiltonian also diverges. Using the

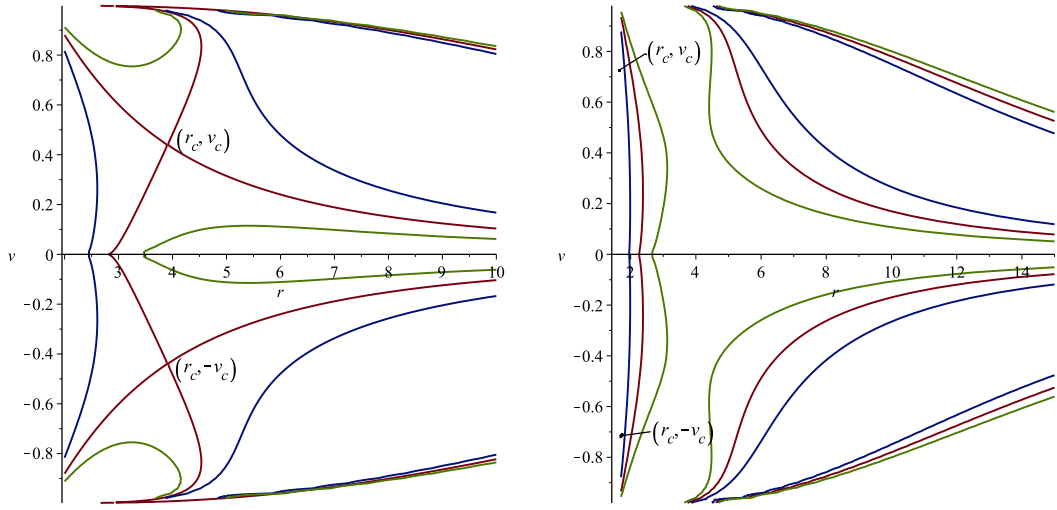


Figure 4: Left Panel: Contour plot of (71) for KS RBH with  $b = 0.9$ ,  $M = 1$ ,  $\alpha = 0.5$ ,  $Y = -1/8$  and  $n_c = 0.19$ . The parameters are  $r_h \simeq 1.666666667$ ,  $r_c \simeq 3.928297284$  and  $v_c \simeq 0.4377733181$ . The Solution curve passing the the CP  $(r_c, v_c)$  for  $H = H_c \simeq 0.3173998409$ . Right Panel: Contour plot of (71) for DDF BH with  $q = 0.5$ ,  $M = 1$ ,  $\alpha = 0.5$ ,  $Y = -1/8$  and  $n_c = 0.19$ . The parameters are  $r_h \simeq 1.614278177$ ,  $r_c \simeq 1.988815258$  and  $v_c \simeq 0.7359530796$ . The Solution curve avoiding the CP  $(r_c, v_c)$  for  $H = H_c \simeq 0.2143193585$ .

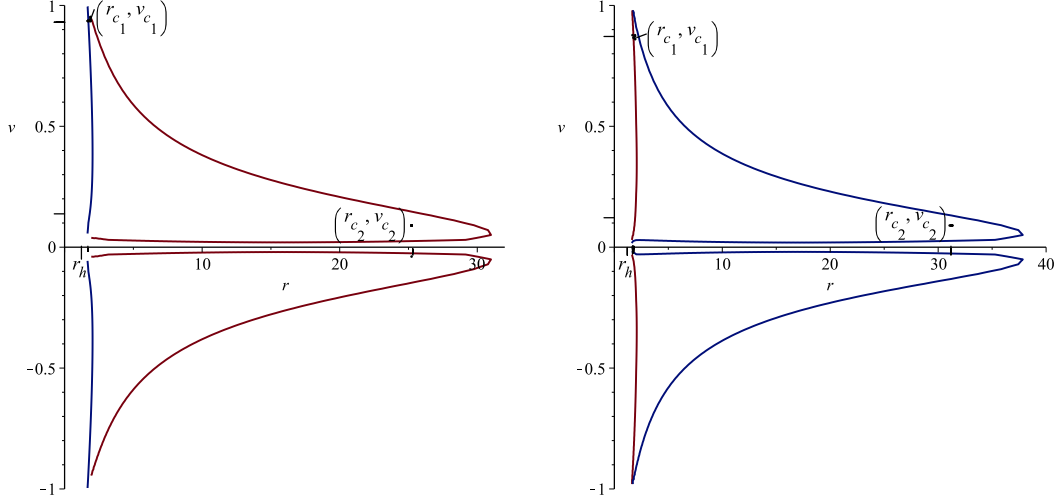


Figure 5: Left Panel: Contour plot of (71) for KS RBH with  $b = 0.9$ ,  $M = 1$ ,  $\alpha = 1.9$ ,  $Y = 1/8$  and  $n_c = 0.001$ . The parameters are  $r_h \simeq 1.666666667$ ,  $r_{c_1} \simeq 1.719016508$ ,  $v_{c_1} \simeq 0.9439334159$ ,  $r_{c_2} \simeq 25.49303509$  and  $v_{c_2} \simeq 0.1443387155$ . Red plot is the solution curve passing through  $(r_{c_2}, v_{c_2})$  and  $(r_{c_2}, -v_{c_2})$  with  $H = H_{c_2} = 0.9452241039$ . Blue plot is the solution curve passing through  $(r_{c_1}, v_{c_1})$  and  $(r_{c_1}, -v_{c_1})$  with  $H = H_{c_2} = .2028972112$ . Right Panel: Contour plot of (71) for DDF RBH with  $q = 0.5$ ,  $M = 1$ ,  $\alpha = 1.8$ ,  $Y = 1/8$  and  $n_c = 0.001$ . The parameters are  $r_h \simeq 1.614278177$ ,  $r_{c_1} \simeq 1.724674282$ ,  $v_{c_1} \simeq 0.8893889966$ ,  $r_{c_2} \simeq 31.59490067$  and  $v_{c_2} \simeq 0.1283035425$ . Blue plot is the solution curve passing through  $(r_{c_2}, v_{c_2})$  and  $(r_{c_2}, -v_{c_2})$  with  $H = H_{c_2} = 0.9576657920$ . Red plot is the solution curve passing through  $(r_{c_1}, v_{c_1})$  and  $(r_{c_1}, -v_{c_1})$  with  $H = H_{c_2} = 0.2585395967$ .

technique of authors [31, 32], we finally come to the following system

$$(\alpha - 1 - v_c^2) \left( \frac{1 - v_c^2}{r_c^4 X(r_c) v_c^2} \right)^{(\alpha-1)/2} = \frac{n_c}{2Y} (r_c^5 X(r_c)_{r_c})^{\frac{1}{2}} v_c^2, \quad (72)$$

$$v_c^2 = \frac{r_c X(r_c)_{r_c}}{r_c X(r_c)_{r_c} + 4X(r_c)}. \quad (73)$$

By putting Eq.(73) in (72), we find  $r_c$  and then corresponding  $v_c$  from (73). It is observed from Eq.(72) that  $\alpha < 1$ ,  $v_c^2 > \alpha - 1$  as mentioned in [31]. The left panel of Figure 4 represents the contour plot of (71) for KS BH with  $b = 0.9$ ,

$M = 1$ ,  $\alpha = 0.5095$ ,  $Y = -1/8$  and  $n_c = 0.19$ . We find the new behavior of the fluid by finding the exact CP  $r_c \simeq 3.928297284$ ,  $v_c \simeq 0.4377733181$  for which  $H = H_c \simeq 0.3173998409$ . It can be observed that the accretion starts from subsonic flow for  $r \rightarrow \infty$  then follow supersonic passing through the saddle point and ends into the horizon. However, the supersonic flow out observed in the vicinity of horizon passing through the saddle point and ends subsonically for  $r \rightarrow \infty$ . The right panel of Figure 4 represents the contour plot of (71) for DDF RBH with  $q = 0.5$ ,  $M = 1$ ,  $\alpha = 0.5$ ,  $Y = -1/8$  and  $n_c = 0.19$ . We find the CP at  $r_c \simeq 1.988815258$ ,  $v_c \simeq 0.7359530796$  for which  $H = H_c \simeq 0.2143193585$ . We notice that the accretion starts from subsonic flow for  $r \rightarrow \infty$  then follow supersonic avoiding the saddle point and ends into the horizon. However, the supersonic flow out observed in the vicinity of horizon avoiding the saddle point and ends subsonically for  $r \rightarrow \infty$ . These features agrees with GR BHs [31, 32].

In Fig. 5, we are assuming  $\alpha = 1.9$ ,  $Y = 1/8$ ,  $n_c = 0.001$  in left panel for KS RBH and  $\alpha = 1.8$ ,  $Y = 1/8$ ,  $n_c = 0.001$  in right panel for DDF RBH which lead to four CPs for each RBH, but none of them is saddle point. There are three types of flow: (1) non heteroclinic because the solution curves avoiding the CPs and accretion starting from leftmost point until the horizon, (2) followed by non relativistic flow out and (3) subsonic non-global. There are two other fluids flow: (1) partly subsonic accretion and flow-out with source-sink at rightmost point of both graphs and (2) partly supersonic accretion and flow-out with source-sink at rightmost point of both graphs. Other solutions could also be found at  $\alpha = 1.8$  for KS RBH and at  $\alpha = 5.5/3$  for DDF RBH. Since the fluid is considered as a test matter in geometry of BH, we observe no homoclinic flow i.e. flow following closed path [31, 32].

## 7 Conclusion

In this work, we studied the steady state spherically symmetric accretion onto RBHs. Applying the technique of [31, 32] and develop the Hamiltonian dynamical system for tackling the accretion problem. As the pressure, baryon number density and other densities which diverge on horizon, while three velocity have remained bounded by  $-1$  and  $1$  and hence it does not diverge on horizon. We have studied the motion of isothermal relativistic, ultra-relativistic, radiation and sub-relativistic test fluids in the frame work of Hamiltonian dynamical system around RBHs. The thermodynamical prop-

erties of fluids have been studied for different choices of EoS parameter. Moreover, CPs and conserved quantities have been found for different fluids. The behavior of accreting fluid have been discussed as subsonic and supersonic according to EoS and RBHs. We compared the fluid flow for two different RBHs and observed that the fluid flow and CPs are closer to DDF RBH instead of KS RBH (Figure 1). If CP is the saddle point then the solution curve divides the  $(r, v)$  plane into the regions where fluid flow is physical for higher values of Hamiltonian and unphysical in lower values of Hamiltonian.

It has been observed that the supersonic accretion followed by subsonic accretion ends inside the horizon and it does not give support to the claim that "the flow must be supersonic at the horizon" [48]. Hence the flow of the fluid is neither transonic nor supersonic near the horizon [49, 50]. These new solutions correspond to fine tuning and instability problems in dynamical systems. Furthermore, we have observed from Figure 3 that if the value of EoS parameter ( $k$ ) increases then CPs shifted **towards both RBHs**. Hence, it is concluded that the three velocity depends on CPs and EoS parameter on phase space. It is interesting to mention here that the results obtain in Figure 1 agrees with [31, 32]. We have also observed from right panel of Figure 4 that accretion starts from subsonic and ends at supersonic into horizon but avoiding the saddle points for DDF RBH. Hence no saddle point occurs in the solution of DDF RBH. Furthermore, the subsonic flow appears to be almost non-relativistic. These features agrees with GR BHs [31, 32]. On the other hand, in left panel of Figure 4, it is seen that accretion starts from subsonic and ends at supersonic into horizon but passing through the saddle points for KS RBH. Hence, saddle point occurs in the solution of KS RBH. These features are different from [31, 32].

## Acknowledgment

We are thankful to the anonymous referees for the constructive remarks on our manuscript which have improved our manuscript. We are also thankful to Prof. Olivier Sarbach for useful discussions and remarks on our manuscript.

## References

- [1] Chaverra, E. and Sarbach, O.: *Class. Quant. Grav.* **32**, 15 (2015).

- [2] Jawad, A. and Shahzad, M. U.: Eur. Phys. J. C **76**, 123 (2016).
- [3] Elizalde, E. and Hildebrandt, S. R.: Phys. Rev. D **65**, 124024 (2002).
- [4] Zaslavskii, O. B.: Phys. Lett. B **688**, 278 (2010).
- [5] Hawking, S.W. and Ellis, G.F.: The Large Scale Structure of SpaceTime (Cambridge Univ. Press 1973).
- [6] Senovilla, J.M.M.: Gen. Relat. Gravit. **30**, 701 (1998).
- [7] Bardeen, J. M., in Abstracts of the 5th International Conference on Gravitation and the Theory of Relativity, edited by V. A. Fock et al. (Tbilisi University Press, Tbilisi, 1968), p. 174.
- [8] Ayn-Beato, E., Garca, A.: Phys. Rev. Lett. **80**, 5056 (1998).
- [9] Borde, A.: Phys. Rev. D **50**, 3692 (1994).
- [10] Borde, A.: Phys. Rev. D **55**, 7615 (1997)
- [11] Hayward, S.A.: Phys. Rev. Lett. **96**, 031103 (2006).
- [12] Berej, W., Matyjasek, J., Tryniecki, D., Woronowicz, M.: Gen. Relativ. Gravit. **38(5)**, 885906 (2006).
- [13] Leonardo, B. et al.: Phys. Rev. D **90**, 124045 (2014).
- [14] Kehagias, A. and Sfetsos, K.: Phys. Lett. **B678**, 123 (2009).
- [15] Bondi, H.: MNRAS **112**, 195 (1952).
- [16] Karkowski, J. and Malec, E.: Phys. Rev. D **87**, 044007 (2013).
- [17] Mach, P. and Malec, E.: Phys. Rev. D **88**, 084055 (2013).
- [18] Mach, P., Malec, E., Karkowski, J.: Phys. Rev. D **88**, 084056 (2013).
- [19] Michel, F. C.: Astrophys. Space Sci. **15**, 153 (1972).
- [20] Moncrief, V.: Astrophys. J. **235**, 1038 (1980).
- [21] Babichev, et al., E.: Phys. Rev. Lett. **93**, 021102 (2004).

- [22] Guzman, F. S. and Lora-Clavijo, F. D.: MNRAS **415**, 225 (2011).
- [23] Malec, E.: Phys. Rev. D **60**, 10403 (1999).
- [24] Lora-Clavijo, F. D., Gracia-Linares, M. and Guzman, F. S.: MNRAS **443**, 2242 (2014).
- [25] Ananda, D. B., Bhattacharya, S. and Das, T. K.: General Relativity and Gravitation **47**, 96 (2015).
- [26] Pun, C. S. J. at el.: Phys. Rev. D **78**, 024043 (2008).
- [27] Chakraborty, S.: Class. Quant. Grav. **32**, 075007 (2015).
- [28] Gonzalez, J., A. and Guzman, F., S.: Phys. Rev. D **79**, 121501 (2009).
- [29] Debnath, U.: Eur. Phys. J. C **75**, 129 (2015).
- [30] Bahamonde, S. and Jamil, M.: Eur. Phys. J. C **75**, 508 (2015).
- [31] Ahmed at el.: Eur. Phys. J. C **76**, 269 (2016).
- [32] Ahmed at el.: Eur. Phys. J. C **76**, 280 (2016).
- [33] Rezzolla, L. and Zanotti, O.: Relativistic Hydrodynamics Oxford University Press, Oxford (2013).
- [34] Chaverra, E. and Sarbach, O.: AIP Conf. Proc. **1473**, 54 (2011).
- [35] Chaverra, E., Morales, M. D. and Sarbach, O.: Phys. Rev. D **91**, 104012 (2015).
- [36] Chaverra, E., Mach, P. and Sarbach, O.: Class. Quant. Grav. **33**, 10 (2016).
- [37] Mu-In Park: JHEP **0909**, 123 (2009).
- [38] Horava, P.: Phys. Lett. **B694**, 172 (2010); Horava, P.: JHEP **0903**, 020 (2009); Horava, P.: Phys. Rev. D **79**, 084008 (2009); Horava, P.: Phys. Rev. Lett. **102**, 161301 (2009).
- [39] Harko, T., Kovacs, Z., Lobo, F. N. S.: Proceedings of the Royal Society of London A: Mathematical, Physical and Engineering Sciences (2010).

- [40] Myung, Y. S.: Phys. Lett. **B685**, 318 (2010); Konoplya, R. A.: Phys. Lett. **B679**, 499 (2009)
- [41] Iorio, L., Ruggiero, M. L.: Int. J. Mod. Phys. D **20**, 1079 (2011).
- [42] Eune, M., Gwak, B., Kim, W.: Phys. Lett. **B718**, 1505 (2013).
- [43] Culetu, H.: Astrophys. Space Sci. **2**, 360(2015).
- [44] Dagun, C.: Economie Appliquee. **30**, 413 (1977).
- [45] Leonardo, Balart and Elias, C. Vagenas: Phys. Rev. D **90**, 124045 (2014).
- [46] Dymnikova, I.: Class. Quant. Grav. **19**, 725 (2002).
- [47] Ayon-Beato, E. and Garcia, A.: Phys. Rev. Lett. **80**, 5056 (1998).
- [48] Chakrabarti, S.K.: Int. J. of Mod. Phys. D **20**, 1723 (2011).
- [49] Novikov, I., Thorne, K.S.: in Black Holes, ed. by C. DeWitt, B. DeWitt (Gordon and Breach, New York, 1973), p. 343
- [50] Chakrabarti, S.K.: Theory of transonic astrophysical flows (World Scientific, Singapore, 1990).
- [51] Nagle, R.K., Saff, E.B., Snider, A.D.: Fundamentals of differential equations and boundary value problems, 6th edn. (Pearson, International Edition, UK, 2012).
- [52] Polking, J., Boggess, A., Arnold, D.: Differential equations with boundary value problems, 2nd edn. (Prentice Hall, Upper Saddle River, 2006).
- [53] Bugl, P.: Differential Equations: Matrices and Models (Prentice Hall, Englewood Cliffs, 1995).
- [54] Azreg-Anou, M.: Class. Quantum Grav. **30**, 205001 (2013).